Transient binding of an activator BH3 domain to the Bak BH3-binding groove initiates Bak oligomerization

Haiming Dai,[1] Alyson Smith,[2] X. Wei Meng,[1] Paula A. Schneider,[1] Yuan-Ping Pang,[2] and Scott H. Kaufmann[1,2]

[1]Division of Oncology Research, Department of Oncology and [2]Department of Molecular Pharmacology and Experimental Therapeutics, Mayo Clinic, Rochester, MN 55905

The mechanism by which the proapoptotic Bcl-2 family members Bax and Bak release cytochrome *c* from mitochondria is incompletely understood. In this paper, we show that activator BH3-only proteins bind tightly but transiently to the Bak hydrophobic BH3-binding groove to induce Bak oligomerization, liposome permeabilization, mitochondrial cytochrome *c* release, and cell death. Analysis by surface plasmon resonance indicated that the initial binding of BH3-only proteins to Bak occurred with similar kinetics with or without detergent or mitochondrial lipids, but these reagents increase the strength of the Bak–BH3-only protein interaction. Point mutations in Bak and reciprocal mutations in the BH3-only proteins not only confirmed the identity of the interacting residues at the Bak–BH3-only protein interface but also demonstrated specificity of complex formation in vitro and in a cellular context. These observations indicate that transient protein–protein interactions involving the Bak BH3-binding groove initiate Bak oligomerization and activation.

Introduction

The Bcl-2 protein family regulates cellular life and death decisions by controlling mitochondrial outer membrane (MOM) permeabilization (MOMP), a key step in the intrinsic apoptotic pathway (Cory and Adams, 2002; Jiang and Wang, 2004; Kroemer et al., 2007; Youle and Strasser, 2008; Chipuk et al., 2010). Current models indicate that Bax and Bak, which directly cause MOMP, are regulated by other family members. In particular, antiapoptotic proteins, such as Bcl-2, Bcl-x_L, and Mcl-1, inhibit MOMP, whereas members of the BH3-only subfamily promote MOMP.

A previous study has suggested that BH3-only proteins can be further subdivided into two classes (Letai et al., 2002). Direct activators are thought to bind Bax or Bak directly and initiate their oligomerization (Walensky et al., 2006; Kim et al., 2009). In contrast, sensitizers are thought to bind only to antiapoptotic Bcl-2 family members, thereby inhibiting neutralization of Bax, Bak, and the direct activators. Based on a variety of observations, including the ability of synthetic BH3 peptides to trigger Bax-mediated permeabilization of isolated mitochondria (Letai et al., 2002) or liposomes (Kuwana et al., 2005), pull-down assays performed using recombinant proteins (Kim et al., 2009), and studies of apoptosis induction in cells lacking various BH3-only family members (e.g., Ren et al., 2010), Bim, truncated Bid (tBid; a caspase 8–generated Bid fragment), and Puma are classified as direct activators, whereas Bad is viewed as a prototypic sensitizer. The role of other BH3-only proteins, such as Noxa, is somewhat less clear, with some studies concluding that they are sensitizers (Letai et al., 2002; Kuwana et al., 2005; Kim et al., 2006; Ren et al., 2010) and other results suggesting that they are direct activators (Du et al., 2011).

Despite the central importance of Bax and Bak in apoptotic responses, their activation also remains incompletely understood (Reed, 2006; Kroemer et al., 2007; Youle and Strasser, 2008; Dewson and Kluck, 2009; Chipuk et al., 2010). Three distinct models of Bax activation have been proposed. One postulates that Bax is intrinsically active unless inhibited by cytosolic binding partners or antiapoptotic Bcl-2 family members (Willis et al., 2007). A second suggests that activator BH3-only proteins, which have been modeled by stapled BH3 peptides, bind near the Bax N terminus to induce an active Bax conformation

Correspondence to Scott H. Kaufmann: Kaufmann.scott@mayo.edu

Abbreviations used in this paper: BMH, bismaleimidohexane; CGM, conjugate gradient minimization; FPLC, fast protein liquid chromatography; LUV, large unilamellar vesicle; MEF, mouse embryonic fibroblast; MMDS, multiple molecular dynamics simulation; MOM, mitochondrial outer membrane; MOMP, MOM permeabilization; NMR, nuclear magnetic resonance; NTA, nitrilotriacetic acid; SDM, steepest descent minimization; SPR, surface plasmon resonance; tBid, truncated Bid; wt, wild type.

The Rockefeller University Press $30.00
J. Cell Biol. Vol. 194 No. 1 39–48
www.jcb.org/cgi/doi/10.1083/jcb.201102027

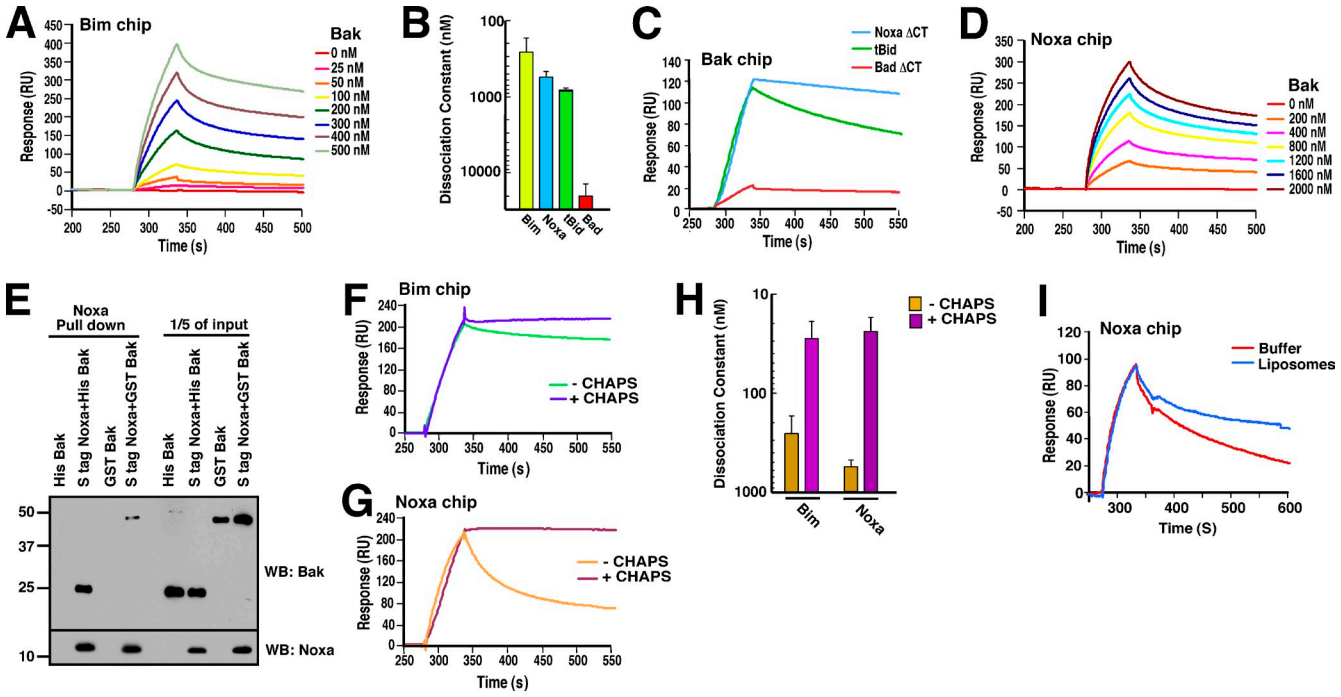

Figure 1. **Direct interaction of Bim_{EL}, tBid, and Noxa with Bak.** (A and D) SPR (relative units [RU]) of immobilized full-length wt human Bim_{EL} (A) or Noxa (D) exposed to increasing concentrations of purified BakΔTM. (B) K_ds of various BH3-only proteins and BakΔTM calculated from SPR assays. Error bars are ± SD of three independent experiments using different chips and protein preparations. (C) SPR of immobilized BakΔTM exposed to 200 nM purified NoxaΔCT, BadΔCT, or tBid. (E) Purified S peptide–Noxa was mixed with His_6-Bak or GST-Bak and then recovered on S protein–agarose as described in the Materials and methods. The pull-downs and one-fifth of the inputs were subjected to SDS-PAGE and immunoblotting. Molecular masses are given in kilodaltons. (F and G) SPR of immobilized full-length wt Bim_{EL} (F) or Noxa (G) exposed to purified BakΔTM in buffer ± 1% CHAPS. (H) K_ds in the absence or presence of CHAPS. Error bars are ± SD of three experiments using different protein preparations. (I) Effect of mitochondrial lipids on Noxa–Bak binding. WB, Western blot.

(Walensky et al., 2006; Gavathiotis et al., 2008; Kim et al., 2009). A third indicates that initial binding of activator BH3-only proteins to MOM lipids is followed by interaction with Bax, leading to Bax membrane insertion, oligomerization, and MOMP (Lovell et al., 2008; Montessuit et al., 2010).

It is unclear how well any of these models explains Bak activation. Unlike Bax, Bak is constitutively associated with the MOM in the absence of activator proteins (Wei et al., 2000; Antonsson et al., 2001). Moreover, Bak oligomerization appears to be triggered by interactions involving its BH3 domain and α6 helix (Dewson et al., 2008, 2009) rather than binding of activators to the α1 helix as described for Bax (Gavathiotis et al., 2008).

The present study was designed to identify steps leading to Bak activation. In particular, we set out to assess the interaction of direct activators with Bak, identify the protein domains involved, and evaluate the role of lipid in modulating these interactions. Here, we demonstrate for the first time that Bak oligomerization, subsequent MOMP, and Bak-mediated killing in intact cells involve transient interactions of BH3-only proteins with the Bak BH3-binding groove.

Results and discussion

Interactions between direct activators and Bak

Using surface plasmon resonance (SPR), a technique that examines interactions between proteins over time (Jason-Moller et al., 2006; Berggård et al., 2007), we observed a dose-dependent increase in the binding of Bak to immobilized Bim (Fig. 1 A) with a mean dissociation constant (K_d) of 260 nM (Fig. 1 B). Importantly, this Bim–Bak interaction occurred in the absence of lipids, suggesting that Bak binds directly to Bim. In addition, Bak bound tBid, another direct activator, but not the sensitizer Bad (Fig. 1, B and C). Interestingly, Bak also bound Noxa as detected by SPR (Fig. 1, B–D) and in vitro pull-down assays (Fig. 1 E).

To assess the influence of a hydrophobic environment on these interactions, we introduced the zwitterionic detergent CHAPS. This addition had little effect on the initial binding of Bak to Bim (Fig. 1 F) or Noxa (Fig. 1 G), suggesting that protein–protein interactions drive the initial BH3-only protein–Bak association. CHAPS did, however, markedly slow dissociation of complexes once they formed, reducing the mean K_ds of the Bim–Bak and Noxa–Bak complexes to 29 and 24 nM, respectively (Fig. 1 H). Similar effects were observed with MOM lipids (Fig. 1 I).

Direct activator–Bak interactions involve the Bak BH3-binding groove

To identify the domains responsible for complex formation, mutations were introduced into the binding partners. Changing three hydrophobic residues of Noxa (L29, F32, and L36) to Glu (Noxa 3E; Fig. 2 A) or the conserved residues L29 and D34 to Ala (Noxa 2A) markedly diminished the Noxa–Bak

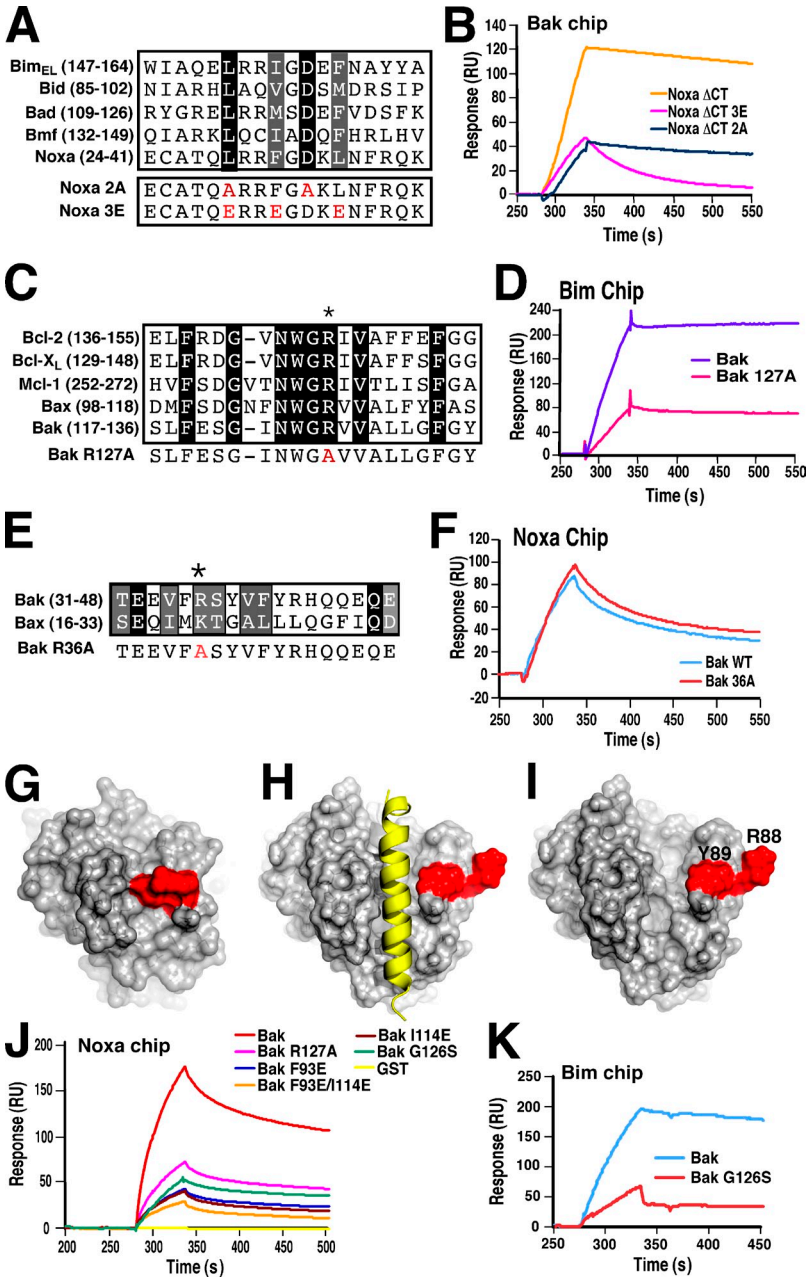

Figure 2. **BH3 domain–Bak interactions involve the Bak BH3-binding groove.** (A) Sequence alignment of selected human BH3 domains. Residues marked in red are mutated in NoxaΔCT 3E and NoxaΔCT 2A. (B) SPR (relative units [RU]) of immobilized BakΔTM exposed to 200 nM purified NoxaΔCT, NoxaΔCT 3E, or NoxaΔCT 2A. (C) Sequence alignment of selected human BH1 domains. The asterisk indicates the conserved BH3-binding groove Arg that is critical for the function of antiapoptotic family members (Sattler et al., 1997). (D) SPR (relative units) of immobilized full-length Bim$_{EL}$ exposed to 200 nM BakΔTM or BakΔTM R127A in CHAPS. (E) Alignment of Bax and Bak showing Bax Lys21 (asterisk) implicated in BH3 peptide binding. (F) SPR of immobilized Noxa exposed to 400 nM BakΔTM or BakΔTM R36A. (G) Top view of Bak structure (Moldoveanu et al., 2006) used as a starting point for docking the Noxa BH3 domain and performing MDDSs. Note the blockage of the BH3-binding groove by Y89^{Bak} and R88^{Bak} (red). (H) Top view of Noxa (in helix model) in complex with Bak (in surface model). (I) Top view of Bak in the bound state showing conformational changes of Y89^{Bak} and R88^{Bak} to vacate the Noxa-binding groove with two hydrophobic holes. (J) SPR of immobilized Noxa exposed to 800-nM fusions of GST with Bak, Bak 127A, Bak G126S, Bak 93E, Bak 114E, Bak 93E/114E, or GST alone. (K) SPR of immobilized full-length Bim$_{EL}$ exposed to 200 nM BakΔTM or BakΔTM G126S. In panels A, C, and E, identical residues are indicated by black shading, and similar residues are shown by gray shading.

interaction (Fig. 2 B), indicating that binding involves the Noxa BH3 domain. In addition, mutation of Bak R127, a conserved residue in the BH3-binding groove of all multidomain Bcl-2 family members (Fig. 2 C), to Ala markedly diminished binding to Bim (Fig. 2 D) or Noxa (see next paragraph). In contrast, mutation of Bak R36, which corresponds to a residue reported to be critical for binding of activator peptides to Bax (Gavathiotis et al., 2008), had no effect on the BH3-only protein–Bak interaction (Fig. 2, E and F). These results suggested that BH3-only proteins bind to the Bak BH3-binding groove.

To further study the BH3 domain–Bak interaction, we used homology modeling and multiple molecular dynamics simulations (MMDSs) to generate a model of a BH3-only protein–Bak complex, which was then validated experimentally. Noxa was used for model building (Fig. 2, G–I) because its smaller size permitted adequate conformational sampling, although both Bim and Noxa were used (Fig. 2, J and K) to confirm predictions of the model. The SWISS-MODEL program (Kiefer et al., 2009) predicted that residues 19–45 of human Noxa (Hijikata et al., 1990; Oda et al., 2000) adopt an α-helical conformation. Superimposition of a Bak monomer (derived from crystal structure of the dimer; Moldoveanu et al., 2006) over nuclear magnetic resonance (NMR) structure of the Mcl-1 BH3-binding groove, a known binding site for Noxa, suggested that Bak has a similar binding groove composed of α3 and α4 helices (residues 81–98 and 105–120), whereas this groove is blocked by R88 and Y89 (Fig. 2 G) in free monomeric Bak. After the helical Noxa fragment was manually docked into the blocked Bak groove, the crude Noxa–Bak model was refined by

72 10-ns molecular dynamics simulations (Pang, 2004), collectively offering samplings for 0.72 µs (see Materials and methods; Table S1 and Table S2). In the resulting MMDS-refined model, Bak R88 and Y89 vacate the groove (Fig. 2 H), and the helical Noxa fragment binds with L29 and L36 plugged into two hydrophobic holes (Fig. 2 I). This model predicts that several additional residues in the Bak BH3-binding groove interact with Noxa (Fig. S1), including Bak G126 (hydrogen bonding to Noxa N37 and Q40), I114 (van der Waals interactions with Noxa C25 and L29), and F93 (π–π interaction with Noxa F32). Mutation of these key residues, like mutation of R127, diminished binding of Bak to Noxa (Fig. 2 J) or Bim (Fig. 2 K), further establishing the importance of the Bak BH3-binding groove in interactions with BH3-only proteins.

Direct activator–BH3-binding groove interactions lead to Bak oligomerization

In further experiments, size exclusion fast protein liquid chromatography (FPLC) was used to assess Bak oligomerization state. All of these experiments included CHAPS to simulate a lipid environment and potentially stabilize BH3-only protein–Bak interactions (Fig. 1 H). In the absence of BH3-only proteins, Bak migration was consistent with its monomer molecular mass of 25 kD (Fig. 3 A, top). Bad, which binds Bak poorly (Fig. 1), had no effect on Bak mobility (Fig. 3 A, bottom). In contrast, Bim, tBid, or Noxa shifted Bak to a new peak of M_r ∼200,000 (Fig. 3, B–F, red boxes). This shift occurred within 20 min (Fig. 3 D) and was evident upon prolonged incubation even when the Noxa/Bak ratio was 1:10 (Fig. 3 F). Although the BH3-only proteins were absent from this peak of M_r ∼200,000 at later times (Fig. 3, B, C, E, and F, green boxes), an intermediate complex was detected at earlier times (Fig. 3 D, orange box), suggesting that a transient interaction between BH3-only proteins and Bak leads to Bak oligomerization. Conditions that inhibited oligomerization, such as omission of CHAPS (not depicted) or dithiothreitol (Fig. 3 G, left), also allowed detection of stable complexes in pull-down assays (Figs. 1 E and 3 G, right). The Noxa 2A and 3E mutants with diminished Bak binding (Fig. 2 B) failed to trigger Bak oligomerization (Fig. 3 H and not depicted), highlighting the role of the activator BH3 domain in Bak activation. Moreover, oligomerization was abolished by the Bak R127A mutation (Fig. 3 I) but not R36A mutation (Fig. 3 J), demonstrating critical involvement of the Bak BH3-binding groove in Bak oligomerization.

Contribution of BH3 domain–Bak interactions to Bak-mediated membrane permeabilization

Immunoprecipitations performed with an antibody that recognizes the N terminus of Bak in its active conformation (Griffiths et al., 2001) suggested that Bak had been activated by BH3-only protein binding in vitro (Fig. 4 A). To further assess this issue, the ability of Bak to permeabilize membranes was examined using liposomes composed of MOM lipids (Kuwana et al., 2005; Pitter et al., 2008) supplemented with DGS-nitrilotriacetic acid (NTA)-Ni (Oh et al., 2010), purified Bak protein lacking its transmembrane domain but containing a C-terminal His_6 epitope for membrane tethering, and synthetic BH3 peptides (Fig. 4 B). In this system, Bak-mediated liposome permeabilization (monitored by release of fluoresceinated dextran) was enhanced by the wild-type (wt) Bim or Noxa BH3 peptide but not the Bad or mutant Noxa BH3 peptide (Fig. 4, C–E), paralleling the ability of these peptides to oligomerize Bak (Fig. 4 F). Further experiments compared Bak G126S, which displays diminished BH3-only protein binding (Fig. 2, J and K) and oligomerization, with Bak G126S/N86G, which has a reciprocal mutation that restores oligomerization (Dewson et al., 2008). Importantly, wt Bim BH3 peptide failed to facilitate membrane permeabilization by either mutant (Fig. 4, G and H). Introduction of a reciprocal N160G mutation in the Bim BH3 domain, which enhances the binding to Bak G126S/N86G (see next section), selectively facilitated liposome permeabilization by Bak G126S/N86G, which can oligomerize, but not wt Bak or Bak G126S (Fig. 4, G and H). Collectively, these results demonstrate the importance of both BH3 domain–Bak BH3-binding groove interactions and Bak oligomerization in membrane permeabilization.

To further examine the function of the BH3 protein–induced Bak oligomers, we added Bak, Bim, and/or Noxa to mitochondria from $Bax^{-/-}Bak^{-/-}$ mouse embryonic fibroblasts (MEFs). Although Bak, Bim, or Noxa alone did not induce MOMP, Bim + Bak or Noxa + Bak did (Fig. 4 I). Because the BakΔTM used in this experiment lacks a transmembrane domain, these results not only provide further evidence that Bim and Noxa activate Bak in vitro but also suggest that tethering of Bak to the membrane through its C terminus is potentially dispensable for MOM disruption.

Requirement of activator BH3 domain–Bak BH3-binding groove interactions for Bak-mediated killing

To evaluate BH3-only protein–Bak interactions in a cellular context, $Bax^{-/-}Bak^{-/-}$ MEFs were reconstituted with wt Bak, Bak G126S (not able to bind activator BH3-only proteins; Fig. 2, J and K), or Bak N86G/G126S (containing a reciprocal mutation to potentially allow Bak to oligomerize; Dewson et al., 2008). All constructs contained the transmembrane domain to mimic the native protein as closely as possible. Immunoblotting confirmed expression of these proteins at roughly endogenous levels in two independent clones (Fig. 5 A). Reconstituted MEFs were then transiently transfected with Bim or Noxa constructs at ∼90% transfection efficiency, plated, and allowed to form colonies. Under conditions that resulted in equivalent expression of transfected constructs (Fig. S2 A), wtBim and wtNoxa had no effect on $Bax^{-/-}Bak^{-/-}$ MEFs. Conversely, these constructs diminished the colony formation of cells expressing wtBak (Fig. 5 B), confirming the requirement for Bak in the antiproliferative effects of Bim and Noxa in this system. The Bak G126S mutation, which markedly diminished binding to BH3-only proteins and membrane permeabilization (Figs. 2, J and K; and 4 H), abolished the cytotoxicity of both Bim and Noxa (Fig. 5 B). Moreover, wtBim and wtNoxa were unable to kill cells reconstituted with Bak N86G/G126S (Fig. 5 B), further suggesting that direct interaction of Bim or Noxa with Bak

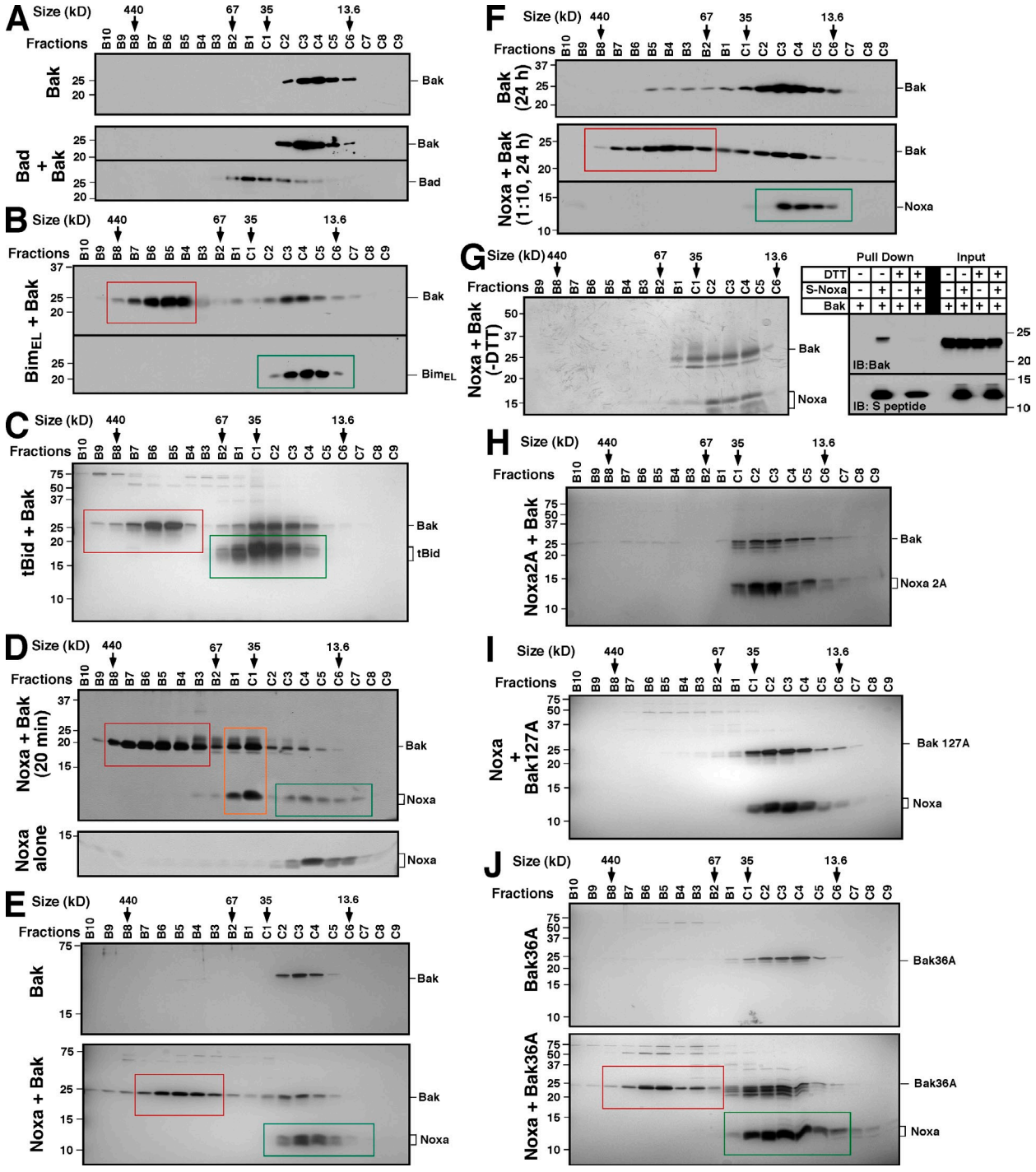

Figure 3. **Bak oligomerization depends on BH3 domain–BH3-binding groove interactions.** Reactions containing purified Bak (A–H), Bak R127A (I), or Bak R36A (J) alone or with a threefold molar excess of Bad (A), Bim$_{EL}$ (B), tBid (C), Noxa (D, E, G, I, and J), or Noxa 2A (H) or a 1:10 molar ratio of Noxa to Bak (F) was incubated for 20 min (D), 24 h (F), or 1 h (other panels) at 23°C in the absence (G) or presence of DTT (all other panels) and then subjected to pull-down and blotting (G, right) or applied to a Superdex S200 column (other panels). Column fractions were subjected to SDS-PAGE, transferred to nitrocellulose, and blotted (A, B, and F) or silver stained (other panels). Arrows indicate size markers. Red boxes show oligomerized Bak. Green boxes show monomeric BH3-only proteins in reactions in which Bak oligomerized. The orange box shows transient intermediate complexes.

is required for the antiproliferative effect. Importantly, however, introduction of a reciprocal mutation into the BH3 domain of either Noxa or Bim (Noxa N37G or Bim N160G) not only enhanced binding to Bak N86G/G126S (Fig. S2 B) and membrane permeabilization (Fig. 4, G and H) but also restored the cytotoxicity of the BH3-only proteins in a cellular context (Fig. 5 B).

Implications for Bak activation

The aforementioned results presented provide new insight into several aspects of Bak activation. First, our observations indicate that interactions between BH3 domains of activator proteins and the Bak BH3-binding groove initiate Bak oligomerization. This conclusion is based on the ability of mutations in the activator

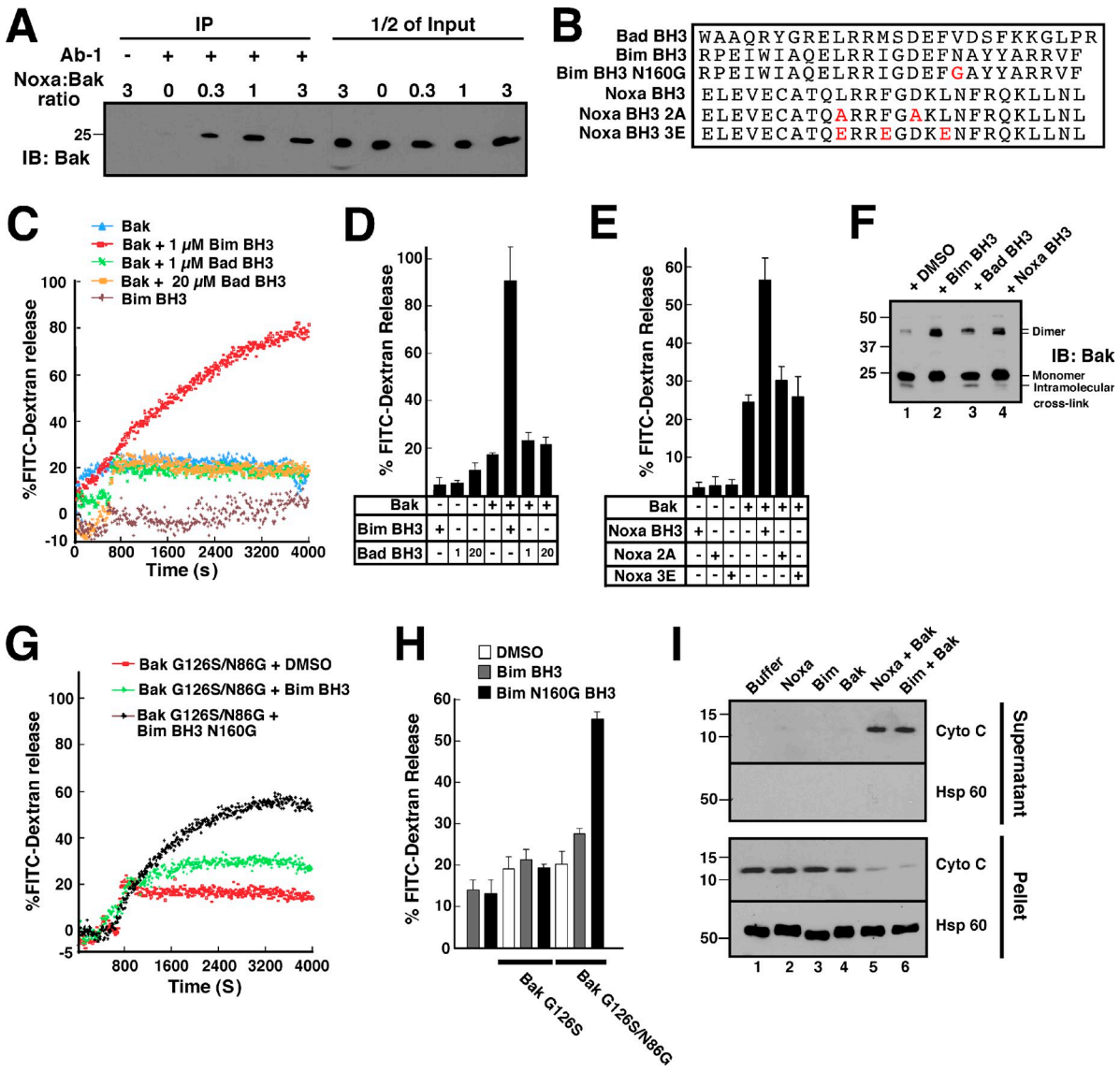

Figure 4. **Bak membrane permeabilization depends on BH3 domain–BH3-binding groove interactions.** (A) Purified Bak and Noxa at the indicated molar ratios were incubated for 1 h in the presence of CHAPS and captured using antiactive Bak Ab-1 precoupled to protein A/G–agarose. Immunoprecipitates and half of the inputs were blotted with an antibody against total Bak. (B) Peptides used to trigger Bak activation in vitro. Residues mutated in various peptides are indicated in red. (C–E) FITC–dextran 10 encapsulated in LUVs containing 5% DGS-NTA-Ni was incubated with 500 nM (C and D) or 1 μM (E) His_6-BakΔCT along with 1 μM Bim BH3 peptide, 1 or 20 μM Bad BH3 peptide, or 2 μM of the indicated Noxa BH3 peptide. FITC-dextran release was measured as a function of time (C) or calculated at 4,000 s from three independent experiments (D and E). Error bars are means ± SD. (F) Liposomes were incubated with 500 nM Bak and the indicated BH3 peptide (1 μM) at 37°C for 30 min, then cross-linked with 100 μM BMH, and analyzed. (G and H) Liposomes were incubated with 2 μM His_6-BakΔCT G126S or His_6-BakΔCT N86G/G126S in the absence or presence of a 10-fold molar excess of the indicated Bim BH3 peptide. FITC-dextran release was measured as a function of time (G) or calculated at 4,000 s from two independent experiments (H). (I) After mitochondria from *Bax*$^{-/-}$*Bak*$^{-/-}$ MEFs were incubated with purified proteins for 1 h, sedimented, and washed, the supernatant and pellet were blotted for cytochrome *c* (Cyto C) and mitochondrial Hsp60. Molecular masses are given in kilodaltons. IP, immunoprecipitation; IB, immunoblot.

BH3 domain or Bak BH3-binding groove to diminish binding, Bak oligomerization, membrane permeabilization, and cytotoxicity as well as the ability of reciprocal mutations in the BH3 domain of the activator and BH3-binding groove of Bak to restore these functions. These results are in contrast to Bax, in which BH3-only proteins reportedly bind the α1 helix to initiate oligomerization.

Second, taking advantage of the ability of SPR to assess association and dissociation separately, we observed that the initial association of BH3-only proteins with Bak was unaffected by the CHAPS or MOM lipid. Instead, these reagents strengthened the BH3 domain–BH3-binding groove interactions once they occurred and facilitated subsequent events. These results are again in contrast to Bax, in which BH3-only proteins are currently thought to interact with MOM lipids before binding Bax.

Third, the present results provide evidence that BH3-only protein–Bak interactions are transient. Although the possibility of a transient interaction has been previously suggested (Wei et al., 2000) because of the poor recovery of activator BH3-only proteins with Bak from apoptotic cells, tBid, Bim, and Puma have more recently been pulled down after incubation with Bax or Bak in vitro (Kim et al., 2009). Our observations help resolve this apparent contradiction. In the absence of CHAPS or DTT, Bak does

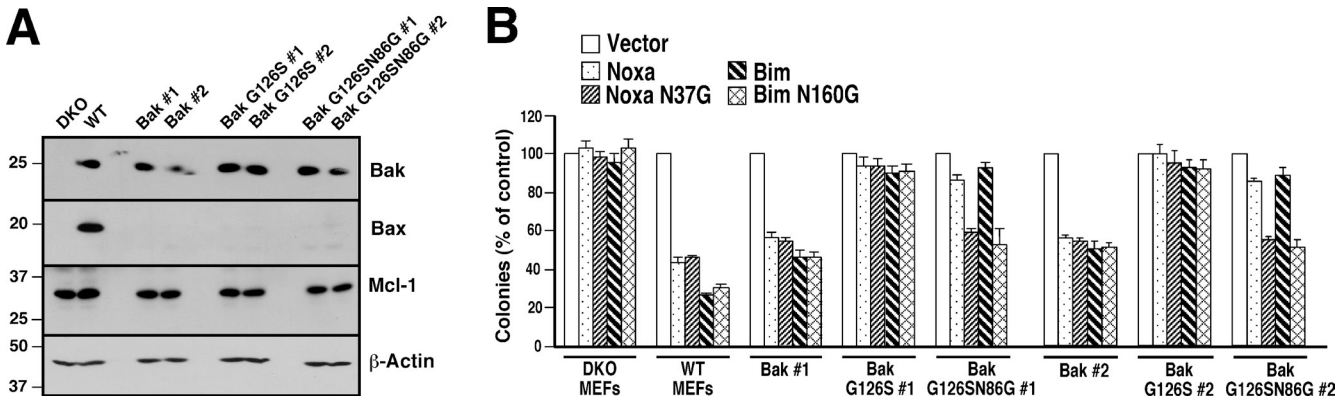

Figure 5. **Bim- and Noxa-induced cytotoxicity depends on BH3 domain–BH3-binding groove interactions.** (A) Whole-cell lysates prepared from wt MEFs, *Bax*$^{-/-}$*Bak*$^{-/-}$ MEFs or *Bax*$^{-/-}$*Bak*$^{-/-}$ MEFs reconstituted with the indicated Bak constructs were harvested for immunoblotting. #1 and #2 represent independent clones. Molecular masses are given in kilodaltons. (B) MEFs were transfected with empty vector or the indicated BH3-only protein and assayed for colony formation. The number of colonies obtained from cells transfected with control plasmid (pSPN) was set to 100%. Error bars are means ± SD of three independent experiments. DKO, double knockout.

not form oligomers, and the interaction with a BH3-only protein is stable enough for pull-down or SPR assays (Figs. 1 and 3 G). If Bak is immobilized in this monomeric state, CHAPS or lipids strengthen this interaction with activator BH3-only proteins. When Bak is not immobilized, however, these strong interactions appear to trigger Bak oligomerization, which is accompanied by ejection of the activator protein from the oligomers (Fig. 3), accounting for previous difficulties in detecting this interaction during apoptosis in vivo. These observations are again in contrast to Bax, as the latter reportedly remains associated with activator BH3-only proteins upon oligomerization in vitro.

Finally, the present results provide evidence that Noxa is a direct Bak activator. In particular, Noxa (like Bim) binds Bak tightly but transiently, oligomerizes Bak in vitro, and induces Bak-mediated MOMP. Importantly, the cytotoxicity of Noxa in Bak-expressing cells is abolished by mutation of residues responsible for Noxa–Bak complexation and restored by reciprocal mutations in the two partners (Fig. 5). This identification of Noxa as a direct Bak activator provides an explanation for the recent observation that 30,000 Noxa molecules per cell can be cytotoxic even though antiapoptotic Bcl-2 binding partners are 3- to 10-fold more abundant (Smith et al., 2011).

In summary, the present results demonstrate that the kinetics of BH3-only protein–Bak interactions can be studied using SPR in vitro, that Bak oligomerization is initiated by transient binding of an activator BH3 domain to the Bak BH3-binding groove, that Noxa (like tBid or Bim) can serve as a Bak activator, and that these interactions regulate life and death in intact cells, as indicated by the effects of reciprocal mutations in Bim or Noxa and Bak. Collectively, the present observations suggest that Bak activation differs substantially from current models of Bax activation summarized in the Introduction.

Materials and methods

Materials

Reagents were obtained as follows: lipids and extruder from Avanti Polar Lipids, Inc., CM5 biosensor chips from GE Healthcare, Polysorbate 20 from Biacore AB, glutathione from Sigma-Aldrich, bismaleimidohexane (BMH) and glutathione-agarose from Thermo Fisher Scientific, and S protein–agarose and Ni^{2+}-NTA-agarose from EMD. Antibodies to the following antigens were purchased from the indicated suppliers: Hsp60, Bim, Bad, and Mcl-1 from Cell Signaling Technology; cytochrome *c* and Mcl-1 from BD; Noxa from Enzo Life Sciences; active Bak (Ab-1) from EMD; Bax and Bak from Millipore; and actin (goat polyclonal) from Santa Cruz Biotechnology, Inc. Anti–S peptide antibody was raised in our laboratory as previously described (Hackbarth et al., 2004). BH3 peptides were generated by solid-phase synthesis in the Mayo Clinic Proteomics Research Center.

Protein expression and purification

Human Bcl-2 family members were evaluated in this study. cDNAs encoding Noxa (available from GenBank/EMBL/DDBJ under accession no. NM_021127) and Noxa lacking the C-terminal domain (NoxaΔCT; residues 1–40) were cloned into pET29a(+) to yield constructs with an N-terminal S peptide epitope tag and C-terminal His_6 tag. Plasmids encoding BakΔTM (GenBank accession no. BC004431; residues 1–186) in pET29b(+) and pGEX-4T-1 (Moldoveanu et al., 2006) were gifts from Q. Liu and K. Gehring (McGill University, Montreal, Canada). cDNAs encoding Bim_{EL} (GenBank accession no. AF032457), tBid (GenBank accession no. AF042083; residues 61–195), and Bad (GenBank accession no. AF021792) or Bad lacking the C-terminal domain (BadΔCT; residues 1–149) were cloned into pET29a(+) to yield constructs with N-terminal S peptide epitope tags and C-terminal His_6 tags. Plasmids encoding Bak mutants and Noxa mutants were generated using site-directed mutagenesis. All plasmids were subjected to automated sequencing to verify the described alteration and confirm that no additional mutations were present.

Plasmids were transformed into *Escherichia coli* BL21 by heat shock. After cells were grown to an optical density of 0.8, IPTG was added to 1 mM, and incubation was continued for 24 h at 16°C (His_6-Bak, GST-Bak, and mutants) or 3 h at 37°C (Noxa, Bim_{EL}, Bad, tBid, and mutants). Bacteria were then washed and sonicated intermittently on ice in calcium- and magnesium-free Dulbecco's PBS containing 1 mM PMSF (GST-tagged proteins) or TS buffer (150 mM NaCl containing 10 mM Tris-HCl, pH 7.4, and 1 mM PMSF; His_6-tagged proteins). All further steps were performed at 4°C. His_6-tagged proteins were applied to Ni^{2+}-NTA-agarose, and columns were washed with 20 vol TS buffer followed by 10 vol TS buffer containing 40 mM imidazole and then eluted with TS buffer containing 200 mM imidazole. GST-tagged proteins were then incubated with glutathione-agarose for 4 h at 4°C, and beads were washed twice with 20–25 vol PBS and eluted with PBS containing 20 mM reduced glutathione for 30 min at 4°C.

SPR

Proteins for SPR were further purified by FPLC on Superdex S200 (GE Healthcare), concentrated in a centrifugal concentrator (Centricon; Millipore), dialyzed against Biacore buffer (10 mM Hepes, pH 7.4, 150 mM NaCl, 0.05 mM EDTA, and 0.005% [wt/vol] Polysorbate 20), and stored at 4°C for <48 h before use. Binding assays were performed at 25°C on a biosensor (Biacore 3000; Biacore) using His_6-Bim_{EL} or His_6-Noxa immobilized on a CM5 chip and Biacore buffer containing GST or GST-BakΔTM (wt or

mutant) injected at 30 µl/min for 1 min. Bound protein was allowed to dissociate in Biacore buffer at 30 µl/min for 10 min and then desorbed with 2 M $MgCl_2$. Binding kinetics were derived using BIAevaluation software (Biacore). Similarly, GST-BakΔTM on a CM5 chip was exposed to tBid, BadΔCT, or NoxaΔCT and its mutants. In some experiments, Biacore buffer contained 1% CHAPS or large unilamellar vesicles (LUVs) as indicated in the figure legends.

S peptide pull-down
Purified GST-BakΔTM or His_6-BakΔTM and S peptide–Noxa were incubated in PBS with 5 mM DTT at 23°C for 1 h and bound to S protein–agarose at 4°C for 12 h. After four washes with PBS, proteins eluted in SDS sample buffer were subjected to SDS-PAGE and immunoblotting.

Analytical gel filtration
Purified His_6-Bak and BH3-only protein were mixed in CHAPS buffer (1% CHAPS, 1% glycerol, 150 mM NaCl, 5 mM DTT, and 20 mM Hepes, pH 7.5) at 23°C for 1 h. 200-µl samples were subjected to FPLC at 4°C on Superdex S200. 500-µl fractions were analyzed by SDS-PAGE followed by silver staining or immunoblotting. For calibration, molecular markers (Sigma-Aldrich) in CHAPS buffer were run through the same column.

Immunoprecipitation
After purified Bak and Noxa were incubated in CHAPS buffer (1% CHAPS, 1% glycerol, 150 mM NaCl, and 20 mM Hepes, pH 7.5) with 5 mM DTT at 30°C for 1 h, immunoprecipitations were performed for 1 h at 4°C using 5 µg antiactive Bak Ab-1 that was precoupled to protein A/G–agarose beads using dimethyl pimelimidate. After four washes with isotonic wash buffer containing 1% CHAPS, bound proteins were solubilized in SDS sample buffer, subjected to SDS-PAGE, and probed with antibodies that recognize total Bak.

Preparation of FITC-dextran lipid vesicles
1-Palmitoyl-2-oleoyl-*sn*-glycero-3-phosphocholine, 1-palmitoyl-2-oleoyl-*sn*-glycero-3-phosphoethanolamine, L-α-phosphatidyl-inositol, cardiolipin, cholesterol, and 18:1 DGS-NTA-Ni at a weight ratio of 36:22:9:8:20:5 were dried as thin films in glass test tubes under nitrogen and then under vacuum for 16 h. To encapsulate FITC-labeled dextran 10 (F-d10; Invitrogen), 50 mg lipid in 1 ml of 20-mM Hepes and 150-mM KCl, pH 7.0, buffer was mixed with 50 mg F-d10, sonicated, and extruded 15 times through a 100-nm polycarbonate membrane. Untrapped F-d10 was removed by gel filtration on Sephacryl S-300 HR (GE Healthcare). Phosphate was determined by colorimetric assay (Abcam).

Liposome release assay
Release of F-d10 from LUVs was monitored by fluorescence dequenching using a fluorimetric plate reader. After purified His_6-Bak ± BH3 peptide was added to LUVs (final lipid concentration of 10 µg/ml), 96-well plates were incubated at 37°C and assayed (excitation of 485 nm and emission of 538 nm) every 10 s. F-d10 release was quantified by the equation $([F_{sample} - F_{blank}]/[F_{Triton} - F_{blank}] \times 100)$, in which F_{sample}, F_{blank}, and F_{Triton} are fluorescence of reagent-, buffer-, and 1% Triton X-100–treated LUVs (modified from Oh et al., 2010).

Cytochrome *c* release
Purified His_6-Noxa, His_6-Bim_{EL}, and His_6-Bak were dialyzed against mitochondria buffer (150 mM KCl, 5 mM $MgCl_2$, 1 mM EGTA, 25 mM Hepes, pH 7.5) and diluted into mitochondria buffer with 5 mM DTT. Mitochondria purified from *Bak*$^{-/-}$*Bax*$^{-/-}$ MEFs (Goping et al., 1998) were incubated with proteins at 23°C for 1 h. After centrifugation at 10,000 *g* for 15 min, supernatants and pellets were analyzed by immunoblotting.

BMH cross-linking
As an alternative to FPLC, Bak oligomers were also analyzed by SDS-PAGE after cross-linking. In brief, 20 µM Bak in HK buffer (20 mM Hepes, 150 mM KCl, pH 7.4) was preincubated with 500 µM DTT for 1 h, then incubated for 30 min at 37°C with liposomes at a final Bak concentration of 500 nM with or without 1 µM synthetic BH3 peptides. BMH was then added to a final concentration of 100 µM (Meng et al., 2007), and cross-linking was allowed to proceed at 23°C for 30 min. After the reaction was stopped by incubation with 5 mM DTT for 15 min, samples were diluted with SDS sample buffer, heated to 65°C for 20 min, separated on 12% (wt/vol) polyacrylamide gels in the presence of SDS, transferred to nitrocellulose, and probed with anti-Bak antibodies.

Stable cell lines
Bak$^{-/-}$*Bax*$^{-/-}$ MEFs (Wei et al., 2001) were transfected with wtBak (nucleotides 1–636) or the indicated mutant in pcDNA3.1/Hygro (Invitrogen) by electroporation using a square wave electroporator (BTX 830; Harvard Apparatus) at 260 mV for 10 ms and, 24 h later, selected with 800 µg/ml hygromycin. Clones were isolated using cloning rings and analyzed by immunoblotting.

Clonogenic assays
After pSPN plasmid (Hackbarth et al., 2004) encoding S peptide–Noxa (ORF nucleotides 1–165), S peptide–Bim_{EL} (ORF nucleotides 1–597), or sequence-verified mutants generated by site-directed mutagenesis were transfected by electroporation (see previous paragraph) along with a plasmid encoding EGFP–histone H2B into *Bak*$^{-/-}$*Bax*$^{-/-}$ MEFs stably expressing wt or mutant Bak, aliquots of 300 cells were plated in replicate 60-mm dishes, allowed to form colonies, and stained. The transfection efficiency, checked by flow cytometry for EGFP 48 h after electroporation, was generally 90%.

Model preparation
The starting structure of Noxa–Bak was generated by manually docking a fragment of human Noxa (residues 19–45) in the α-helical conformation into the Y89-blocked groove of Bak (residues 21–183) taken from the crystal structure of a Bak homodimer (Protein Data Bank accession no. 2IMT; Moldoveanu et al., 2006). This placed $L29^{Noxa}$ near $I114^{Bak}$ and $L118^{Bak}$, $L36^{Noxa}$ near $V129^{Bak}$ and $I85^{Bak}$, and the Noxa helix atop $Y89^{Bak}$. For the Bak domain or the Noxa helix, all His, Glu, Asp, Arg, and Lys residues were treated as HIP, GLU, ASP, ARG, and LYS, respectively. Crystallographically determined H_2O molecules were removed before docking. The topology and coordinate files of the resulting Noxa–Bak complex were generated by the PREP, LINK, EDIT, and PARM modules of AMBER (Assisted Model Building with Energy Refinement) 5.0 (Pearlman et al., 1995). The complex was refined by energy minimization using the SANDER module of AMBER 5.0 with a dielectric constant of 1.0 and 500 cycles of steepest descent minimization (SDM) followed by 10,000 cycles of conjugate gradient minimization (CGM). The docking-generated complex and average complex structure of cluster 6 from first-round simulations (Table S1) were used for first- and second-round simulations, respectively. The energy-minimized complex was solvated with 5,897 and 6,744 TIP3P H_2O molecules (Jorgensen et al., 1983) for the first- and second-round simulations, leading to systems of 20,703 and 23,244 atoms. H_2O molecules were obtained from solvating the complex using a preequilibrated box of 216,000 TIP3P molecules whose hydrogen atomic charge was set to 0.4170, in which any H_2O molecule was removed if it had an O closer than 2.2 Å or an H closer than 2.0 Å to any solute atom or if it was located further than 10.0 Å along the x, y, or z axis from any solute atom.

MMDSs
The solvated complex system was energy minimized for 100 cycles of SDM followed by 100 cycles of CGM to remove close van der Waals contacts in the system, then heated from 0 to 300 K at a rate of 10 K/ps under constant temperature and volume, and finally, simulated independently with a unique seed number for initial velocities at 300 K under constant temperature and pressure using the PMEMD module of AMBER 8.0 (Case et al., 2005) with an AMBER force field (ff99SB; Hornak et al., 2006; Wickstrom et al., 2009). All simulations used (a) a dielectric constant of 1.0, (b) the Berendsen coupling algorithm (Berendsen et al., 1984), (c) a periodic boundary condition at a constant temperature of 300 K and a constant pressure of 1 atmosphere with isotropic molecule-based scaling, (d) the Particle Mesh Ewald method to calculate long-range electrostatic interactions (Darden et al., 1993), (e) a time step of 1.0 fs, (f) the SHAKE bond-length constraints applied to all the bonds involving the H atom, (g) saving the image closest to the middle of the primary box to the restart and trajectory files, (h) formatted restart file, and (i) default values of all other inputs of the PMEMD module.

Simulation analysis
Average structures were obtained as previously described (Ekström et al., 2009). For each of the 20 (round 1) or 52 (round 2) simulations of Noxa–Bak, 200 (round 1) or 100 (round 2) instantaneous conformations were saved at 5-ps (round 1) or 10-ps (round 2) intervals during the last 1-ns period. A total of 4,000 (round 1) or 5,200 (round 2) instantaneous conformations of Noxa–Bak from the 20 (round 1) or 52 (round 2) simulations were subjected to a cluster analysis using the average linkage algorithm (epsilon = 3.0 Å and root mean square on residues 111, 134, 93, and 89

of Bak and residue 32 of Noxa; Shao et al., 2007) in the PTRAJ module of AMBER 10 (Case et al., 2005). Seven (round 1) or two (round 2) clusters of the Noxa–Bak conformations were identified (Table S1). The average conformation of each cluster was energy minimized using the SANDER module of AMBER 5.0 with a dielectric constant of 40 and 500 cycles of SDM followed by 10,000 cycles of CGM. The interaction energy between Noxa and Bak of the energy-minimized complex was then calculated using an in-house program with a dielectric constant of 40 and a nonbonded cutoff of 50,000 Å (Table S2).

Online supplemental material

Fig. S1 shows a close-up view of residues in the Noxa BH3 domain and Bak BH3-binding groove that interact. Fig. S2 shows expression of tagged Bim and Noxa in reconstituted MEFs and analysis of BakΔTM N86G/G126S binding to different Noxa constructs. Table S1 shows the cluster analysis of the first- and second-round MMDSs of the Noxa–Bak complex. Table S2 shows intermolecular interaction energies and root mean square deviations of BH3 domain complexes. Online supplemental material is available at http://www.jcb.org/cgi/content/full/jcb.201102027/DC1.

We thank Q. Liu and K. Gehring for Bak expression plasmids and Deb Strauss for editorial help.

This work was supported, in part, by grants R01 CA69008 and T32 GM072474.

Submitted: 4 February 2011
Accepted: 7 June 2011

References

Antonsson, B., S. Montessuit, B. Sanchez, and J.C. Martinou. 2001. Bax is present as a high molecular weight oligomer/complex in the mitochondrial membrane of apoptotic cells. *J. Biol. Chem.* 276:11615–11623. doi:10.1074/jbc.M010810200

Berendsen, H.J.C., J.P.M. Postma, W.F. van Gunsteren, A. Di Nola, and J.R. Haak. 1984. Molecular dynamics with coupling to an external bath. *J. Chem. Phys.* 81:3684–3690. doi:10.1063/1.448118

Berggård, T., S. Linse, and P. James. 2007. Methods for the detection and analysis of protein-protein interactions. *Proteomics*. 7:2833–2842. doi:10.1002/pmic.200700131

Case, D.A., T.E. Cheatham III, T. Darden, H. Gohlke, R. Luo, K.M. Merz Jr., A. Onufriev, C. Simmerling, B. Wang, and R.J. Woods. 2005. The Amber biomolecular simulation programs. *J. Comput. Chem.* 26:1668–1688. doi:10.1002/jcc.20290

Chipuk, J.E., T. Moldoveanu, F. Llambi, M.J. Parsons, and D.R. Green. 2010. The BCL-2 family reunion. *Mol. Cell*. 37:299–310. doi:10.1016/j.molcel.2010.01.025

Cory, S., and J.M. Adams. 2002. The Bcl2 family: regulators of the cellular life-or-death switch. *Nat. Rev. Cancer*. 2:647–656. doi:10.1038/nrc883

Darden, T.A., D.M. York, and L.G. Pedersen. 1993. Particle Mesh Ewald: An N log(N) method for Ewald sums in large systems. *J. Chem. Phys.* 98:10089–10092. doi:10.1063/1.464397

Dewson, G., and R.M. Kluck. 2009. Mechanisms by which Bak and Bax permeabilise mitochondria during apoptosis. *J. Cell Sci.* 122:2801–2808. doi:10.1242/jcs.038166

Dewson, G., T. Kratina, H.W. Sim, H. Puthalakath, J.M. Adams, P.M. Colman, and R.M. Kluck. 2008. To trigger apoptosis, Bak exposes its BH3 domain and homodimerizes via BH3:groove interactions. *Mol. Cell*. 30:369–380. doi:10.1016/j.molcel.2008.04.005

Dewson, G., T. Kratina, P. Czabotar, C.L. Day, J.M. Adams, and R.M. Kluck. 2009. Bak activation for apoptosis involves oligomerization of dimers via their alpha6 helices. *Mol. Cell*. 36:696–703. doi:10.1016/j.molcel.2009.11.008

Du, H., J. Wolf, B. Schafer, T. Moldoveanu, J.E. Chipuk, and T. Kuwana. 2011. BH3 domains other than Bim and Bid can directly activate Bax/Bak. *J. Biol. Chem.* 286:491–501. doi:10.1074/jbc.M110.167148

Ekström, F., A. Hörnberg, E. Artursson, L.G. Hammarström, G. Schneider, and Y.P. Pang. 2009. Structure of HI-6*sarin-acetylcholinesterase determined by X-ray crystallography and molecular dynamics simulation: reactivator mechanism and design. *PLoS ONE*. 4:e5957. doi:10.1371/journal.pone.0005957

Gavathiotis, E., M. Suzuki, M.L. Davis, K. Pitter, G.H. Bird, S.G. Katz, H.C. Tu, H. Kim, E.H. Cheng, N. Tjandra, and L.D. Walensky. 2008. BAX activation is initiated at a novel interaction site. *Nature*. 455:1076–1081. doi:10.1038/nature07396

Goping, I.S., A. Gross, J.N. Lavoie, M. Nguyen, R. Jemmerson, K. Roth, S.J. Korsmeyer, and G.C. Shore. 1998. Regulated targeting of BAX to mitochondria. *J. Cell Biol.* 143:207–215. doi:10.1083/jcb.143.1.207

Griffiths, G.J., B.M. Corfe, P. Savory, S. Leech, M.D. Esposti, J.A. Hickman, and C. Dive. 2001. Cellular damage signals promote sequential changes at the N-terminus and BH-1 domain of the pro-apoptotic protein Bak. *Oncogene*. 20:7668–7676. doi:10.1038/sj.onc.1204995

Hackbarth, J.S., S.-H. Lee, X.W. Meng, B.T. Vroman, S.H. Kaufmann, and L.M. Karnitz. 2004. S-peptide epitope tagging for protein purification, expression monitoring, and localization in mammalian cells. *Biotechniques*. 37:835–839.

Hijikata, M., N. Kato, T. Sato, Y. Kagami, and K. Shimotohno. 1990. Molecular cloning and characterization of a cDNA for a novel phorbol-12-myristate-13-acetate-responsive gene that is highly expressed in an adult T-cell leukemia cell line. *J. Virol.* 64:4632–4639.

Hornak, V., R. Abel, A. Okur, B. Strockbine, A. Roitberg, and C. Simmerling. 2006. Comparison of multiple Amber force fields and development of improved protein backbone parameters. *Proteins*. 65:712–725. doi:10.1002/prot.21123

Jason-Moller, L., M. Murphy, and J. Bruno. 2006. Overview of Biacore systems and their applications. *Curr. Protoc. Protein Sci.* Chapter 19: Unit 19.13.

Jiang, X., and X. Wang. 2004. Cytochrome C-mediated apoptosis. *Annu. Rev. Biochem.* 73:87–106. doi:10.1146/annurev.biochem.73.011303.073706

Jorgensen, W.L., J. Chandreskhar, J.D. Madura, R.W. Impey, and M.L. Klein. 1983. Comparison of simple potential functions for simulating liquid water. *J. Chem. Phys.* 79:926–935. doi:10.1063/1.445869

Kiefer, F., K. Arnold, M. Künzli, L. Bordoli, and T. Schwede. 2009. The SWISS-MODEL Repository and associated resources. *Nucleic Acids Res.* 37(Suppl. 1): D387–D392. doi:10.1093/nar/gkn750

Kim, H., M. Rafiuddin-Shah, H.C. Tu, J.R. Jeffers, G.P. Zambetti, J.J. Hsieh, and E.H. Cheng. 2006. Hierarchical regulation of mitochondrion-dependent apoptosis by BCL-2 subfamilies. *Nat. Cell Biol.* 8:1348–1358. doi:10.1038/ncb1499

Kim, H., H.C. Tu, D. Ren, O. Takeuchi, J.R. Jeffers, G.P. Zambetti, J.J. Hsieh, and E.H. Cheng. 2009. Stepwise activation of BAX and BAK by tBID, BIM, and PUMA initiates mitochondrial apoptosis. *Mol. Cell*. 36:487–499. doi:10.1016/j.molcel.2009.09.030

Kroemer, G., L. Galluzzi, and C. Brenner. 2007. Mitochondrial membrane permeabilization in cell death. *Physiol. Rev.* 87:99–163. doi:10.1152/physrev.00013.2006

Kuwana, T., L. Bouchier-Hayes, J.E. Chipuk, C. Bonzon, B.A. Sullivan, D.R. Green, and D.D. Newmeyer. 2005. BH3 domains of BH3-only proteins differentially regulate Bax-mediated mitochondrial membrane permeabilization both directly and indirectly. *Mol. Cell*. 17:525–535. doi:10.1016/j.molcel.2005.02.003

Letai, A., M.C. Bassik, L.D. Walensky, M.D. Sorcinelli, S. Weiler, and S.J. Korsmeyer. 2002. Distinct BH3 domains either sensitize or activate mitochondrial apoptosis, serving as prototype cancer therapeutics. *Cancer Cell*. 2:183–192. doi:10.1016/S1535-6108(02)00127-7

Lovell, J.F., L.P. Billen, S. Bindner, A. Shamas-Din, C. Fradin, B. Leber, and D.W. Andrews. 2008. Membrane binding by tBid initiates an ordered series of events culminating in membrane permeabilization by Bax. *Cell*. 135:1074–1084. doi:10.1016/j.cell.2008.11.010

Meng, X.W., S.H. Lee, H. Dai, D. Loegering, C. Yu, K. Flatten, P. Schneider, N.T. Dai, S.K. Kumar, B.D. Smith, et al. 2007. Mcl-1 as a buffer for pro-apoptotic Bcl-2 family members during TRAIL-induced apoptosis: a mechanistic basis for sorafenib (Bay 43-9006)-induced TRAIL sensitization. *J. Biol. Chem.* 282:29831–29846. doi:10.1074/jbc.M706110200

Moldoveanu, T., Q. Liu, A. Tocilj, M. Watson, G. Shore, and K. Gehring. 2006. The X-ray structure of a BAK homodimer reveals an inhibitory zinc binding site. *Mol. Cell*. 24:677–688. doi:10.1016/j.molcel.2006.10.014

Montessuit, S., S.P. Somasekharan, O. Terrones, S. Lucken-Ardjomande, S. Herzig, R. Schwarzenbacher, D.J. Manstein, E. Bossy-Wetzel, G. Basañez, P. Meda, and J.C. Martinou. 2010. Membrane remodeling induced by the dynamin-related protein Drp1 stimulates Bax oligomerization. *Cell*. 142:889–901. doi:10.1016/j.cell.2010.08.017

Oda, E., R. Ohki, H. Murasawa, J. Nemoto, T. Shibue, T. Yamashita, T. Tokino, T. Taniguchi, and N. Tanaka. 2000. Noxa, a BH3-only member of the Bcl-2 family and candidate mediator of p53-induced apoptosis. *Science*. 288:1053–1058. doi:10.1126/science.288.5468.1053

Oh, K.J., P. Singh, K. Lee, K. Foss, S. Lee, M. Park, S. Lee, S. Aluvila, M. Park, P. Singh, et al. 2010. Conformational changes in BAK, a pore-forming proapoptotic Bcl-2 family member, upon membrane insertion and direct evidence for the existence of BH3-BH3 contact interface in BAK homo-oligomers. *J. Biol. Chem.* 285:28924–28937. doi:10.1074/jbc.M110.135293

Pang, Y.-P. 2004. Three-dimensional model of a substrate-bound SARS chymotrypsin-like cysteine proteinase predicted by multiple molecular

dynamics simulations: catalytic efficiency regulated by substrate binding. *Proteins*. 57:747–757. doi:10.1002/prot.20249

Pearlman, D.A., D.A. Case, J.W. Caldwell, W.S. Ross, T.E. Cheatham III, S. DeBolt, D. Ferguson, G. Seibel, and P.A. Kollman. 1995. AMBER, a package of computer programs for applying molecular mechanics, normal-mode analysis, molecular-dynamics and free-energy calculations to simulate the structural and energetic properties of molecules. *Comput. Phys. Commun.* 91:1–41. doi:10.1016/0010-4655(95)00041-D

Pitter, K., F. Bernal, J. Labelle, and L.D. Walensky. 2008. Dissection of the BCL-2 family signaling network with stabilized alpha-helices of BCL-2 domains. *Methods Enzymol.* 446:387–408. doi:10.1016/S0076-6879(08)01623-6

Reed, J.C. 2006. Proapoptotic multidomain Bcl-2/Bax-family proteins: mechanisms, physiological roles, and therapeutic opportunities. *Cell Death Differ.* 13:1378–1386. doi:10.1038/sj.cdd.4401975

Ren, D., H.C. Tu, H. Kim, G.X. Wang, G.R. Bean, O. Takeuchi, J.R. Jeffers, G.P. Zambetti, J.J. Hsieh, and E.H. Cheng. 2010. BID, BIM, and PUMA are essential for activation of the BAX- and BAK-dependent cell death program. *Science*. 330:1390–1393. doi:10.1126/science.1190217

Sattler, M., H. Liang, D. Nettesheim, R.P. Meadows, J.E. Harlan, M. Eberstadt, H.S. Yoon, S.B. Shuker, B.S. Chang, A.J. Minn, et al. 1997. Structure of Bcl-xL-Bak peptide complex: recognition between regulators of apoptosis. *Science*. 275:983–986. doi:10.1126/science.275.5302.983

Shao, J., S.W. Tanner, N. Thompson, and T.E. Cheatham III. 2007. Clustering molecular dynamics trajectories: 1. Characterizing the performance of different clustering algorithms. *J. Chem. Theory Comput.* 3:2312–2334. doi:10.1021/ct700119m

Smith, A.J., H. Dai, C. Correia, R. Takahashi, S.H. Lee, I. Schmitz, and S.H. Kaufmann. 2011. Noxa/Bcl-2 protein interactions contribute to bortezomib resistance in human lymphoid cells. *J. Biol. Chem.* 286:17682–17692. doi:10.1074/jbc.M110.189092

Walensky, L.D., K. Pitter, J. Morash, K.J. Oh, S. Barbuto, J. Fisher, E. Smith, G.L. Verdine, and S.J. Korsmeyer. 2006. A stapled BID BH3 helix directly binds and activates BAX. *Mol. Cell*. 24:199–210. doi:10.1016/j.molcel.2006.08.020

Wei, M.C., T. Lindsten, V.K. Mootha, S. Weiler, A. Gross, M. Ashiya, C.B. Thompson, and S.J. Korsmeyer. 2000. tBID, a membrane-targeted death ligand, oligomerizes BAK to release cytochrome c. *Genes Dev.* 14:2060–2071.

Wei, M.C., W.X. Zong, E.H. Cheng, T. Lindsten, V. Panoutsakopoulou, A.J. Ross, K.A. Roth, G.R. MacGregor, C.B. Thompson, and S.J. Korsmeyer. 2001. Proapoptotic BAX and BAK: a requisite gateway to mitochondrial dysfunction and death. *Science*. 292:727–730. doi:10.1126/science.1059108

Wickstrom, L., A. Okur, and C. Simmerling. 2009. Evaluating the performance of the ff99SB force field based on NMR scalar coupling data. *Biophys. J.* 97:853–856. doi:10.1016/j.bpj.2009.04.063

Willis, S.N., J.I. Fletcher, T. Kaufmann, M.F. van Delft, L. Chen, P.E. Czabotar, H. Ierino, E.F. Lee, W.D. Fairlie, P. Bouillet, et al. 2007. Apoptosis initiated when BH3 ligands engage multiple Bcl-2 homologs, not Bax or Bak. *Science*. 315:856–859. doi:10.1126/science.1133289

Youle, R.J., and A. Strasser. 2008. The BCL-2 protein family: opposing activities that mediate cell death. *Nat. Rev. Mol. Cell Biol.* 9:47–59. doi:10.1038/nrm2308